Journal of Materials Chemistry B

ROYAL SOCIETY OF CHEMISTRY

PAPER

View Article Online
View Journal | View Issue

Cite this: J. Mater. Chem. B, 2023, 11, 4695

Development of a synthesis strategy for sulfamethoxazole derivatives and their coupling with hydrogel microparticles†

Veronika Riedl,[a] Matthias Portius,[a] Lara Heiser,[a] Philipp Riedl,[a] Torsten Jakob,[b] Rosa Gehring,[a] Thorsten Berg[c] and Tilo Pompe*[a]

Sulfonamides were the first synthetic antibiotics broadly applied in veterinary and human medicine. Their increased use over the last few decades and limited technology to degrade them after entering the sewage system have led to their accumulation in the environment. A new hydrogel microparticle based biosensing application for sulfonamides is developed to overcome existing labour-intensive, and expensive detection methods to analyse and quantify their environmental distribution. This biosensing assay is based on the soft colloidal probe principle and requires microparticle functionalization strategies with target molecules. In this study, we developed a step-wise synthesis approach for sulfamethoxazole (SMX) derivatives in high yield, with SMX being one of the most ubiquitous sulfonamide antibiotics. After *de novo* synthesis of the SMX derivative, two coupling schemes to poly(ethylene glycol) (PEG) hydrogel microparticles bearing maleimide and thiol groups were investigated. In one approach, we coupled a cysteamine linker to a carboxyl group at the SMX derivative allowing for subsequent binding *via* the thiol-functionality to the maleimide groups of the microparticles in a mild, high-yielding thiol-ene "click" reaction. In a second approach, an additional 1,11-bis(maleimido)-3,6,9-trioxaundecane linker was coupled to the cysteamine to target the hydrolytically more stable thiol-groups of the microparticles. Successful PEG microparticle functionalization with the SMX derivatives was proven by IR spectroscopy and fluorescence microscopy. SMX-functionalized microparticles will be used in future applications for sulfonamide detection as well as for pull-down assays and screenings for new sulfomethoxazole binding targets.

Received 7th February 2023,
Accepted 23rd April 2023

DOI: 10.1039/d3tb00246b

rsc.li/materials-b

1. Introduction

Sulfamethoxazole (SMX) is one main representative of sulfonamides, one of the oldest and widely used classes of synthetic antibiotics.[1] Today, the application field comprises human as well as veterinary medicine with human medicine being the main SMX application field. Also, in human medicine, it is mostly used in combination with additional antimicrobial molecules like trimethoprim.[2,3] Sulfonamides act bacteriostatic by inhibiting the folate synthesis pathway in bacteria through targeting one of the key enzymes, the dihydropteroate synthase (DHPS).[4] Like other antibiotics, sulfonamides enter the environment by excretion or wrong disposal. Since current wastewater treatment plant techniques are not suited to degrade sulfonamides, they are distributed in the environment where they can accumulate at various locations and are now among the most prevalent and detected antimicrobial contaminants.[5] Current studies indicate the negative impacts of sulfonamides on ecosystems as some sulfonamides, such as SMX, can have a toxic effect on aquatic plants like algae. They are also known to affect microbial community structures and their diversity.[6–8] Furthermore, the presence of sulfonamide in environmental waters leads to their accumulation in aquatic animals that are used in the food industry. Additionally, the wide distribution of antibiotics in the environment accelerates the occurrence of antibiotic resistant bacterial strains, which is already one major threat to global health as stated by the World Health Organization.[5,9]

Because of this, the European commission announced in its technical report from 2020 to include SMX in the next "watch list".[10] However, many studies agree that a precise assessment of SMX effects is not possible without a thorough analysis of its

[a] Leipzig University, Institute of Biochemistry, Johannisallee 21-23, 04103 Leipzig, Germany. E-mail: tilo.pompe@uni-leipzig.de
[b] Leipzig University, Institute of Biology, Johannisallee 21-23, 04103 Leipzig, Germany
[c] Leipzig University, Institute of Organic Chemistry, Johannisallee 29, 04103 Leipzig, Germany

† Electronic supplementary information (ESI) available. See DOI: https://doi.org/10.1039/d3tb00246b

environmental distribution. While standard lab based analytical platforms like high pressure liquid chromatography (HPLC) and mass spectrometry (MS) are readily available to analyse and quantify SMX in environment samples, their labour, cost, and time intensive technology limit a widespread monitoring.[11–13] This raises the need for the development of new, fast, and cost-effective technologies enabling point-of-use analysis to monitor and quantify the distribution of SMX and other antibiotics. Over the last few years, various new approaches for sulfonamide detection were published, covering different methods such as immunochemical detection,[14] colorimetric approaches[15] and electrochemical technologies.[16,17] Other emerging technologies are based on biosensing nano- and microparticles as probes for detection with a broad application field.[18–22]

One of those sensing techniques, the soft colloidal probe (SCP) assay, uses functionalized poly(ethylene glycol) (PEG) hydrogel microparticles as probes. The SCP assay is frequently based on a biomimetic binding principle of the target molecule with naturally occurring binding partners, like biochemical binding of inhibitors to enzymatic binding sites. More precisely, SCPs are functionalized with a target analyte molecule. During the assay, SCPs interact with natural binding partners immobilized on a surface and elastically deform upon binding due to their low stiffness, forming a contact area that can be detected by optical readouts such as reflection interference contrast microscopy (RICM). Based on the basic colloidal particle interaction theory, the contact area can be quantitatively correlated with surface interaction energies.[23] The specific interaction of SCPs with the surface can be competitively inhibited by free analytes in the solution. In this way, the size of the contact area correlates with free target analyte molecules in solution, thus enabling the detection and determination of target analytes in a concentration dependent manner. The SCP assay achieves high sensitivity with the detection range down to 10^{-11} M for detecting the pesticide glyphosate and xenohormones (estrogen derivatives).[24,25] Furthermore, the SCP assay approach proved to be highly selective by excluding cross-reactivity of numerous structurally analogue pesticides and hormones. Performing the SCP assay requires hydrogel microparticles functionalized with the target molecule, capable of binding respective immobilized binding partners on a chip.

To develop a new biosensor for sulfonamide antibiotics based on the SCP technology, which will be addressed in future work, we set off to develop SMX functionalized hydrogel microparticles, considering that SMX is one of the most abundant sulfonamide contaminants in the environment.[26] Coupling SMX to hydrogel microparticles with exposed terminal thiol- and maleimide groups requires chemical modification of SMX, which is challenging using commercially available SMX antibiotics and to our knowledge, has not been performed so far. Sulfonamide antibiotics are designed in analogy to *p*-aminobenzoic acid (*p*ABA) molecular structure, the natural substrate of the DHPS enzyme. By imitating *p*ABA binding, sulfonamides competitively inhibit the DHPS and thus the folate biosynthesis pathways in specific microorganisms.[27,28] Sulfonamide derivatives consist of an aromatic ring with a 4-amino and a 1-sulfamoyl group, differing in the substituents bound to the sulfamoyl group. SMX is characterized by its 5-methylisoxazole ring.[26] Many synthesis approaches for sulfonamide derivatives have already been reported reaching from modifications to predominantly *de novo* synthesis.[28,29] Reactions at the isoxazole ring come with demanding challenges due to ring instability under basic conditions.[30] In contrast to that, a *de novo* synthesis of SMX can be advantageous by using specifically modified constituents commercially available. In our study, we chose a *de novo* synthesis approach to generate SMX derivatives that can be coupled to either the maleimide or the thiol groups of the hydrogel microparticles by using different linkers, to generate SMX-functionalized hydrogel microparticles.

2. Experimental

2.1. Materials

4-(Boc-amino)-benzenesulfonyl chloride (**1**) and 1,11-bis-(maleimido)-3,6,9-trioxoundecan were purchased from abcr GmbH. Methyl-3-amino-1,2-oxazole-5-carboxylate (**2**) was purchased from Enamine Ltd. 4-arm PEG-maleimde (2 kDa) and 4-arm PEG-thiol (2 kDa) used for hydrogel microparticle synthesis were obtained from creative PEGworks. Fluorescein-isothiocyanate (FITC) dye was purchased from Acros Organics. HEPES buffer was used in a concentration of 0.1 M at pH 7.0. Borate buffer was used in a concentration of 0.1 M at pH 9.0. Water was used from a Milli-Q® direct water purification system.

2.2. Synthesis of methyl 3-((4-((*tert*-butoxycarbonyl)amino) phenyl)-sulfonamide)isoxazole-5-carboxylate (3)

4-(Boc-amino)-benzenesulfonyl chloride (**1**, 245.1 mg, 0.84 mmol, 1.2 equiv.) and methyl-3-amino-1,2-oxazole-5-carboxylate (**2**, 99.5 mg, 0.70 mmol, 1.0 equiv.) were dissolved in dry pyridine (2.5 mL) and stirred for 24 h at room temperature (r.t.) (Fig. 1). After that, volatile components were evaporated under reduced pressure. The crude yellow product was purified *via* column chromatography (toluene/ethyl acetate, 9 : 1 to 6 : 4, 2% CH_3COOH) to obtain 257.0 mg (92%) of the desired product **3** as a white solid.

R_f (toluene/ethyl acetate, 9 : 1, v/v, 2% CH_3COOH) = 0.17. ^{1}H NMR (400 MHz, chloroform-d): δ = 7.76 (ddd, J = 8.9, 2.6, 2.0 Hz, 2H), 7.50 (ddd, J = 8.9, 2.6, 2.0 Hz, 2H), 7.29 (s, 1H), 7.14 (s, 1H), 6.72 (s, 1H), 3.96 (s, 3H), 1.52 (s, 9H). ^{13}C NMR (100 MHz, chloroform-d): δ = 161.0, 157.8, 156.7, 152.1, 143.9, 131.6, 128.8, 118.2, 103.0, 82.1, 53.2, 28.4. MS (HR-ESI): m/z = 436.0566 (16%, $[M + K^+]$), 342.0393 (100%, $[M\text{-}C_4H_8 + H^+]$). Calc. mass: 342.0396.

2.3. Synthesis of 3-((4-((*tert*-butoxycarbonyl)amino)phenyl) sulfonamide)-isoxazole-5-carboxylic acid (4)

In step II, the ester functionality of **3** (Fig. 1) was saponified to obtain the carboxylic acid **4**. The synthesis was performed based on the procedure published by Sekirnik (née Measures) *et al.*[31] To this end, **3** (100.0 mg, 0.25 mmol, 1.0 equiv.) was dissolved in tetrahydrofuran (THF)/methanol (10 mL, 1 : 1, *v*/*v*). LiOH (29.9 mg, 1.25 mmol, 5.0 equiv.) was added to the

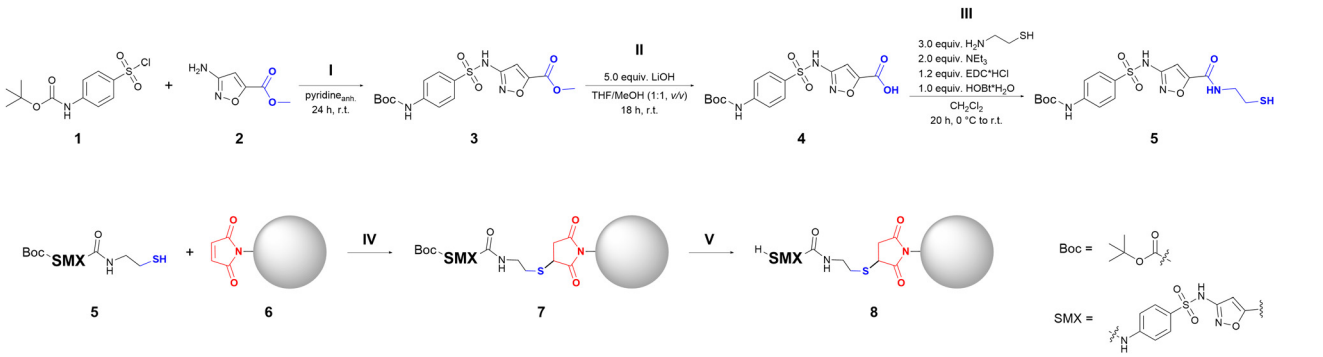

Fig. 1 Overview of the synthesis of the SMX derivative (SMXder) **5** and its coupling to hydrogel microparticles. (upper panel)) All three steps (I–III) of the three-step synthesis of SMXder with the specific compound numbering (see main text) are shown. (lower panel) The two reaction steps (IV and V) of the functionalization of PEG hydrogel microparticles with SMXder are sketched. Functional groups relevant for the coupling of SMXder to PEG microparticles are highlighted in blue for SMXder and red for PEG microparticles.

solution and it was stirred for 18 h at r.t. After that, volatile components were removed under reduced pressure. The crude product was redissolved in water. The pH of the solution was adjusted to pH = 2 using 1 M and 0.1 M HCl. The product was isolated *via* liquid–liquid-extraction using ethyl acetate. The combined organic phases were washed with brine, dried over $MgSO_4$ and filtered. The solution was concentrated under reduced pressure. Water was added to the solution and the rest of the organic solvent was evaporated at 100 mbar and 40 °C. The product precipitated upon cooling the solution to r.t. After filtering and drying in air 75.0 mg (78%) of the desired product **4** was received as a white solid.

In another approach, **4** was synthesized by using the crude yellow product from synthesis step I (**3**) without purification. Reaction steps were performed similar to the above description using **1** (493.1 mg, 1.69 mmol, 1.2 equiv.), **2** (200.0 mg, 1.41 mmol, 1.0 equiv.), dry pyridine (5 mL), THF/methanol (20 mL, 1 : 1, *v*/*v*) and LiOH (168,8 mg, 7.05 mmol, 5.0 equiv.) to obtain 450.2 mg (83%) of the desired product as a white solid.

R_f (toluene/ethyl acetate, 3 : 7, v/v, 2% CH_3COOH) = 0.19. ^{1}H NMR (400 MHz, acetone-d_6): δ = 10.27 (s, 1H), 8.92 (s, 1H), 7.88 (ddd, J = 8.9, 2.6, 2.0 Hz, 2H), 7.76 (ddd, J = 8.9, 2.6, 2.0 Hz 2H), 7.05 (s, 1H), 1.48 (s, 9H). ^{13}C NMR (75 MHz, acetone-d_6): δ = 162.1, 159.2, 157.4, 153.4, 145.6, 133.0, 129.3, 118.7, 103.4, 81.1, 28.4. MS (HR-ESI): m/z = 382.0714 (100%, [M − H$^+$]). Calc. mass: 382.0709.

2.4. Synthesis of *tert*-butyl (4-(*N*-(5-((2-mercaptoethyl)carbamoyl) isoxazol-3-yl)sulfamoyl)phenyl)carbamate (5)

As last step III of the *de novo* synthesis of the SMX derivative, *tert*-butyl (4-(*N*-(5-((2-mercaptoethyl)carbamoyl)isoxazol-3-yl)sulfamoyl)phenyl)carbamate (**5**, Fig. 1) was synthesized. The synthesis was performed based on the procedure published by Pasunooti *et al.*[32] To do so, to a solution of **4** (100.0 mg, 0.26 mmol, 1.0 equiv.) in dichloromethane (DCM) (5 mL) was added to NEt_3 (72.1 µL, 0.52 mmol, 2.0 equiv.), 1-ethyl-3-(3-dimethylaminopopyl) carbodiimide hydrochloride (EDC·HCl) (59.8 mg, 0.31 mmol, 1.2 equiv.) and hydroxybenzotriazole monohydrate (HOBt·H_2O) (39.8 mg, 0.26 mmol, 1.0 equiv.) at 0 °C. After stirring the reaction mixture for 5 min, cysteamine was added (60.2 mg, 0.78 mmol, 3.0 equiv.). The reaction was brought to r.t. and stirred for 20 h. To terminate the reaction, water was added. The mixture was extracted with ethyl acetate. The combined organic phases were washed with brine, dried over $MgSO_4$ and concentrated under vacuum. The crude product was purified *via* column chromatography (ethyl acetate/toluene, 7 : 3, 2% CH_3COOH) or crystallized from the concentrated solution to obtain 64.8 mg (56%) of the desired product as a white solid.

R_f (ethyl acetate) = 0.86. ^{1}H NMR (400 MHz, acetone-d_6): δ = 8.90 (s, 1H), 8.19 (s, 1H), 7.86 (ddd, J = 8.9, 2.6, 2.0 Hz, 2H), 7.75 (ddd, J = 8.9, 2.6, 2.0 Hz, 2H), 6.96 (s, 1H), 3.54 (m, 2H), 2.74 (dt, J = 8.1, 7.0 Hz, 2H), 1.89 (t, J = 8.4 Hz, 1H), 1.48 (s, 9H). ^{13}C NMR (100 MHz, acetone-d_6): δ = 165.0, 159.2, 156.3, 153.3, 145.6, 133.0, 129.3, 118.7, 100.4, 81.1, 43.4, 28.4, 24.1. MS (HR-ESI): m/z = 387.0430 (100%, [M-C_4H_8 + H$^+$]). Calc. mass: 387.0433.

2.5. Synthesis of maleimide-thiol-hydrogel microparticles

The synthesis of maleimide-thiol hydrogel microparticles was performed in accordance with the work of Rettke *et al.*[33] with minor adjustments. Briefly, 4-arm-PEG-thiol (2 kDa) and 4-arm-PEG-maleimide (2 kDa) were dissolved separately in phosphate buffer saline (1×, pH 7.4) to obtain a concentration of 15% (w/w) for each PEG solution. Then, both PEG-solutions were sonicated for 10 min, followed by centrifugation for another 10 min at 16 000*g* and 20 °C. The supernatant was used for further procedure. Afterwards, the polymerization time was set to 40–50 s by adjusting the pH of the 4-arm-PEG thiol solution through NaOH or HCl addition. The polymerization time was determined by mixing 3 µL of each PEG-solution, measuring the time until gelation occurred. The microfluidic setup and synthesis procedure was performed according to Rettke *et al.*[33]

Following the microparticle synthesis, the oil-phase containing a surfactant for particle stabilization during the particle formation process was removed in a washing step by addition of 700 µL 20% 1*H*,1*H*,2*H*,2*H*-perfluorooctanol (PFO) in 3M™ Novec™ 7500 and 500 µL deionized water to the hydrogel microparticle suspension followed by centrifugation at 1840*g* for 1 min at 20 °C. Next, the oil phase was removed, and the washing step was repeated twice whereby only PFO was added.

After the last washing step, the remaining particle suspension was transferred to a larger reaction tube, 10 mL of deionized water was added, and particles were resuspended in a larger volume. The resulting microparticles used in the following experiments were in the size range of 53 μm (particle diameter) with an average contact area diameter size of 4 μm to 5 μm (details see ESI,† Fig. S14 for size distribution and Fig. S16A–C, control condition: particles after synthesis in Millipore water).

2.6. Functionalization of hydrogel microparticles with SMX derivatives

Hydrogel microparticles were either directly functionalized with the SMX derivative or with a 1,11-bis(maleimido)-3,6,9-trioxoundecan linker before SMX derivative functionalization. For direct functionalization, freshly prepared hydrogel microparticles were used up to 1 h after synthesis. First, hydrogel microparticle suspension was transferred to a 1.5 mL Eppendorf Tube® and centrifuged. Centrifugation was performed at 1844*g* and 20 °C for 10 min. The supernatant was removed, and the particles were washed once with 1 mL HEPES buffer.

Then, optionally, 1 mL of a 3 mM 1,11-bis(maleimido)-3,6,9-trioxaundecane linker solution was added and the tubes were placed in a rotating shaker for 1 h at r.t. Samples were centrifuged, the supernatant was removed and particles were washed with 1 mL HEPES buffer. For SMX functionalization, 1 mL of a 6 mM solution of the SMX derivative in acetone/HEPES (1 : 3, v/v) was added. The reaction mixture was agitated for 1 h in a rotating shaker. The tubes were centrifuged, and the supernatant was removed. The particles were washed three times with 1 mL of 4 M HCl. After the last washing step, 1 mL of 4 M HCl was added to the hydrogel microparticles, and the reaction mixture was agitated in a rotating shaker for 4 h at room temperature. The tubes were centrifuged, and the supernatant was removed. Hydrogel microparticles functionalized with the SMX derivative were washed three times with 1 mL water and either directly analysed or stored in water at 4 °C.

2.7. Fourier-transformed infrared spectroscopy (FT-IR)

For FT-IR analysis of functionalized microparticles, 2 μL of the microparticle suspension was applied in a quintuplicate on a silicon microplate. The samples were dried over night at r.t. as well as at 45 °C in a drying chamber right before measurements. Measurements were performed using a Bruker Vector 22 FT-IR spectrometer with a HTS-XT microplate reader. Samples were measured as quintuples in the range of 4000–700 cm^{-1} with a resolution of 4 cm^{-1} and 32 scans per spot. All spectra were baseline-corrected (rubberband method, OPUSlab software v5.0) and averaged.

2.8. Confocal laser scanning microscopy

Samples, containing hydrogel microparticles, were prepared by adding 1 mL of a 10 mM *N*-methyl-maleimide suspension in HEPES buffer. Sample tubes were placed in a rotating shaker for 1 h at r.t. Next, the microparticles were washed once with 1 mL borate buffer. 1 mL of a 256 μM FITC solution in borate buffer was added and samples were placed in a rotating shaker for 1 h at r.t. Lastly, samples were washed three times with 1 mL water. Isopropanol-cleaned cover glasses (d = 13 mm) were placed inside the wells of a 24-well sensor plate with glass bottom (Greiner Bio-One). 300 μL HEPES buffer was presented in each well and 30 μL of the prepared sample was added. Fluorescence images were acquired using a confocal laser scanning microscope (LSM700, Zeiss Microsystems GmbH) equipped with a Plan-Apochromat 10×/0.45 M27 objective (Zeiss Microsystems GmbH). Images were processed using the image analysis software Fiji.[34–36] For this, each z-stack was transformed into a maximum intensity image depicting the maximum grey value (ranging from 0 to 255) for each pixel over the recorded stack of images. The average modal value of the image was calculated. The modal values of each image stack were averaged over all image stacks acquired per well and sample type, respectively.

2.9. Statistics

Data were evaluated and plotted using GraphPad Prism version 8.0.0 for Windows (GraphPad Software, Dotmatics, San Diego, California USA). The plotted data show the mean value with standard deviation, if not stated otherwise. Statistical data were analysed using a non-parametric Kruskal–Wallis test with Dunn's multiple comparison test. Differences were considered significant for $P < 0.001$ (***), $P < 0.002$ (**) and $P < 0.033$(*).

3. Results and discussion

The preparation of the sulfamethoxazole-functionalized hydrogel microparticles can be divided into five steps (Fig. 1), including three steps for the synthesis of the functionalized sulfamethoxazole derivative **5** (dubbed SMXder) (step I to III) and two steps for the functionalization of the hydrogel microparticles (step IV and V). In the following we report the synthesis of SMXder and its analysis by NMR and MS followed by the functionalization procedure of PEG microparticles with SMXder and its analysis by FT-IR and fluorescence microscopy.

3.1. Synthesis of the sulfamethoxazole derivative

The functionalized SMX derivative SMXder (compound **5**, Fig. 1) was synthesized starting from sulfonyl chloride **1** and the primary amine **2**. The *de novo* synthesis provided the opportunity to introduce the desired functionality by using commercially available building blocks. The Boc-protection of the primary amine group of 4-(boc-amino)-benzenesulfonyl chloride (**1**) was necessary to preserve the main scaffold of the SMX derivative, as it is important for binding to its target. The first reaction step is the sulfonamide formation to obtain the Boc-protected, ester-functionalized SMX derivative **3**. Initially, this reaction was performed according to Zhan *et al.*[37] Since the desired product **3** could not be obtained following this procedure, the reaction conditions were adapted. Several test reactions were performed in order to optimize the reaction conditions (ESI† Table S1). Incidentally, in one of the test reactions, a tertiary sulfonamide (compound **3b**, see ESI†) could be isolated, indicating a reaction between the sulfonyl chloride building block **1** and triethylamine (for details see ESI† Section S2). Eventually, the use of anhydrous

pyridine as the auxiliary base, catalyst and solvent was deemed the best (Fig. 1). This way, not only the formation of the side product **3b** could be prevented, but also the solubility of the amine building block **2** could be increased. Furthermore, pyridine can increase the electrophilicity of the sulfonyl chloride **1** by forming an activated pyridinium species.[38] By using an anhydrous solvent, the competing reaction – a fast hydrolysis of the sulfonyl chloride – can be inhibited as well.[39] To prevent coelution of the amine building block **2** and the product **3** during column chromatography, an excess of sulfonyl chloride **1** was used to assure a full conversion of the amine **2**. This way the secondary sulfonamide **3** could be isolated with a yield of 92%.

In the second reaction step II, the ester group of **3** was saponified to generate the free carboxyl acid functionality of compound **4**, which was subsequently used to introduce the bifunctional amino-thiol PEG linker. (Fig. 1). The reaction was performed in accordance with the procedure stated by Sekirnik (née Measures) *et al.* and provided **4** in 78% yield.[31] Saponification of **3** was also successful without its prior purification by column chromatography (Fig. 1, steps I and II), providing the carboxylic acid **4** in an improved overall yield of 83%, further simplifying the synthetic procedure and reducing solvent waste.

Reaction step III, the coupling of the amino-thiol linker, was performed in accordance with the procedure stated by Pasunooti *et al.*[32] The carboxylic acid **4** was equipped with the linker *via* amide coupling. The product could be isolated either by column chromatography or by crystallizing it from the concentrated ethyl acetate solution. The target compound SMXder (**5**) was obtained with a yield of 56%.

The introduction of the thiol linker at this position was chosen, as it is furthest from the main scaffold of the sulfonamide, thereby reducing the possibility of a decreased binding affinity of SMXder (**5**). The short linker length was chosen, as this should give a better tunability of the linker length when introducing a second linker. The thiol functionality was chosen, as it has a better long-term stability than the respective maleimide group.

3.2. Coupling and analysis of the sulfamethoxazole derivative to hydrogel microparticles

PEG-based hydrogel microparticles were prepared by microfluidic synthesis using 4-arm-PEG-thiol (2 kDa) and 4-arm-PEG-maleimide (2 kDa) according to a procedure stated by Rettke *et al.* with minor adjustments.[33] The subsequent preparation of SMXder functionalized hydrogel microparticles **7** was performed by utilizing thiol-ene "click" chemistry, a mild, fast and high-yielding reaction type. To do so, maleimide groups, remaining after the polymerization of the hydrogel microparticles, were initially considered as an option to immobilize the thiol-functionalized SMXder. However, these groups are highly water-susceptible and get readily deactivated upon contact with it. Therefore, only freshly prepared hydrogel microparticles can be used to directly couple SMXder.

This problem can be circumvented by coupling a bis-maleimide linker to the hydrogel microparticles to obtain maleimide functionalized hydrogel microparticles **6**. For that, the more stable thiol groups, remaining after microparticle synthesis, too, are utilized to couple the bis-maleimide linker (Fig. 2A). This way, maleimide groups can be generated on hydrogel microparticles prior to coupling of the thiol-functionalized SMXder (**5**) (Fig. 2B). This procedure also allows for a straightforward adaption of the linker type and length, by exchanging the bis-maleimide linker. As has been previously shown, this can be used to fine-tune the binding affinity of a hydrogel microparticle-coupled molecule to its target binding partner.[40] In the final step, the Boc-protecting group of the immobilized SMXder (**7**) was cleaved under acidic conditions, to obtain the SMX functionalized hydrogel microparticles **8** (Fig. 2B).

Following these arguments, we focused on SMXder coupling using a bifunctional 1,11-bis(maleimido)-3,6,9-trioxaundecane linker. After coupling of SMXder *via* its thiol group, the amino functionality remains accessible, allowing for the investigation of coupling density and homogeneity *via* fluorescence.

By using fluorescein 5(6)-isothiocyanate (FITC), we labelled the amino group and conducted confocal laser scanning microscopy (cLSM) for detection. To avoid cross-reactivity of FITC with unbound thiol-groups on hydrogel microparticles, these groups were masked using 10 mM *N*-methyl maleimide leading to strong reduction of background staining (data not shown).

At first, we investigated a suitable 1,11-bis(maleimido)-3,6,9-trioxaundecane linker concentration that would enable saturation of the particles' surface with SMXder (**5**). For this, we functionalized our hydrogel microparticles with 3 mM and 6 mM linkers, respectively. After SMXder coupling and FITC staining, we

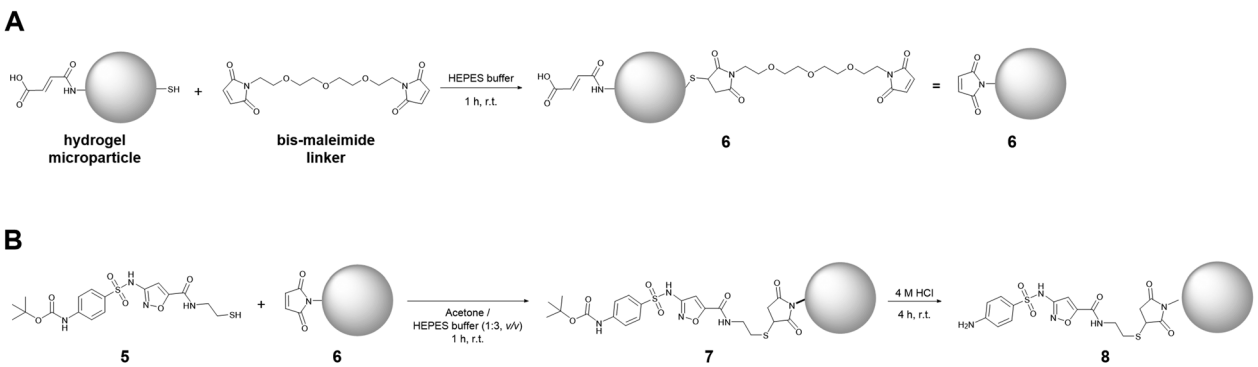

Fig. 2 Sketch of reactions to couple the SMXder (compound **5**) onto PEG hydrogel microparticles and subsequently deprotect it.

observed a slight but significant increase of fluorescence intensity for 6 mM linker concentration (ESI† Fig. S15). Thus, 6 mM linker was used for further SMXder coupling studies. Then, we investigated concentration dependent coupling using 6 μM and 6 mM SMXder. As controls, hydrogel microparticles without a linker and with an attached linker only were used. We observed a significant increase in fluorescence intensity for both SMXder concentrations (0.006 mM and 6 mM) compared to both controls (hydrogel microparticles masked and hydrogel microparticles masked + linker), indicating the successful coupling of SMXder to the particles (Fig. 3). Thereby, no difference in fluorescence intensity between SMXder concentrations of 6 μM or 6 mM was determined, suggesting that saturation of SMXder coupling to hydrogel microparticles was already achieved at 6 μM (Fig. 3E).

It has to be noted, that the homogeneous fluorescence in cLSM images confirms a homogeneous coupling of linkers and SMXder to the particle surface (Fig. 3A–D). To complement the findings from fluorescence microscopy and more specifically detect successful SMXder coupling, transmission FT-IR spectroscopy was performed. Specifically, unmodified and SMXder-functionalized PEG hydrogel microparticles were measured (Fig. 4). To better evaluate the impact of SMXder coupling, differential spectra of modified and unmodified samples were generated by annealing the spectra of both samples *via* the classical least square method followed by a subtraction of the unmodified sample spectrum from the modified one. This way, the strong signal of the thiol-maleimide PEG can be excluded. The differential spectrum clearly shows distinct signals of the SMXder and the 1,11-bis(maleimido)-3,6,9-trioxoundecane linker.

Signals confirming a successful immobilization of the SMXder are especially the absorption between 3500 and 3250 cm^{-1}, as well as the signal at 1650 cm^{-1} indicating the N–H and N–H_2 vibrations of the SMX. Furthermore, the absorption between 1370 and 1330 cm^{-1} and at 1163 cm^{-1} can be assigned to typical vibration signals of sulfamethoxazole[41,42] (Fig. 4). These results match the findings from the fluorescence measurements, confirming the successful coupling of SMXder *via* the bis-maleimide-linker to the hydrogel microparticles.

Taken together, we were able to successfully demonstrate that we established a feasible coupling strategy for the newly synthesized SMXder to hydrogel microparticles. Our work is in agreement with prior works on hydrogel microparticles showing their flexibility and applicability for the coupling of broad spectrum of different analytes. While other works relied on PEG acrylamide particles[24,40,43] we used thiol-maleimide-PEG-particles published earlier by Rettke *et al.*[33] since a thiol-maleimide coupling is stable around pH 7 and compatible with organic buffers such as HEPES, both of which could be necessary for the aspired SCP-Assay for sulfonamide antibiotic detection. Moreover, we investigated, if any of the coupling steps or the solutions necessary for the coupling process affect the structural integrity of the particles (ESI† Fig. S15). By conducting bright field and RICM analyses we detected only small changes regarding particle size and contact area upon adhesion to glass surfaces, respectively. Specifically, the treatment of particles with acetone and 4 M HCl, that was necessary for the functionalization process, led to a slight increase of contact area, suggesting changes in the particle surface

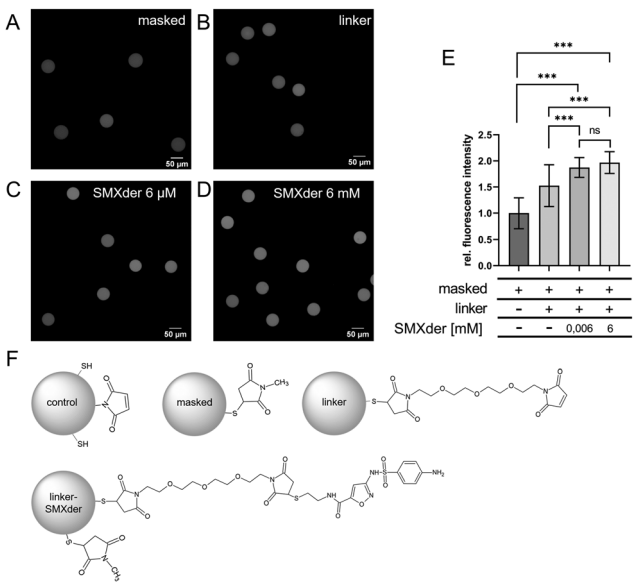

Fig. 3 Fluorescence-based detection of coupled SMXder *via* a bifunctional maleimide linker to hydrogel microparticles. (A) Hydrogel microparticles masked with *N*-methyl maleimide prior to FITC staining. (B) Hydrogel microparticles functionalized with the 1,11-bis(maleimido)-3,6,9-trioxaundecane linker (compound **6**) and masked with *N*-methyl maleimide followed by FITC staining. (C + D) Hydrogel microparticles functionalized with 1,11-bis(maleimido)-3,6,9-trioxaundecane linker followed by coupling 6 μM (C) and 6 mM (D) SMXder (compound 8). Particles were masked with *N*-methyl maleimide followed by FITC staining. (E) Relative fluorescence intensity of at least 140 particles for each condition, normalized to unfunctionalized, masked and FITC-stained hydrogel microparticles (A) and shown as the mean ± SD. *P*-Values of the statistical analysis are indicated as $P < 0.001$ (***), $P < 0.002$ (**), $P < 0.033$(*). (F) Scheme of conditions (A–D) as well as untreated hydrogel microparticles.

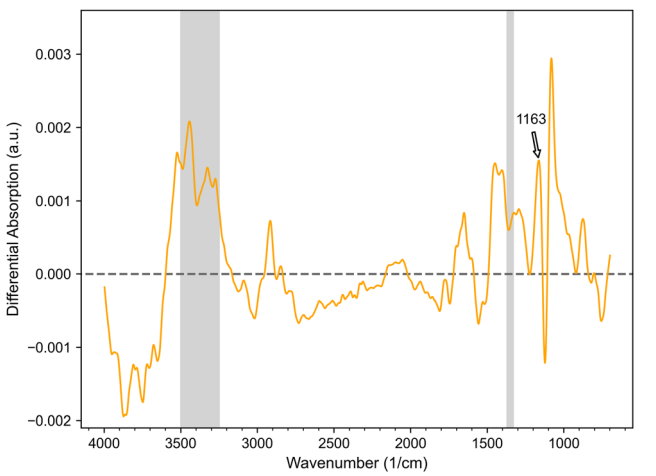

Fig. 4 Differential FT-IR spectrum of SMXder functionalized PEG hydrogel microparticles. The FT-IR signals of neat, unfunctionalized particles and SMXder functionalized particles were annealed *via* the classical least squares method before subtracting the former from the latter. The typical vibration signals of sulfamethoxazole are shaded in grey between 3500 cm^{-1} to 3250 cm^{-1} and 1370–1330 cm^{-1} as well as annotated at 1163 cm^{-1}.

molecular structure (ESI† Fig. S16C). However, the overall structural integrity was not affected in the course of the functionalization process. Thus, SMXder-functionalized hydrogel microparticles can be used as probes in biosensing applications. Moreover, the usability of our approach with organic solvents such as acetone might be of great interest for medical applications or the detection of pharmaceuticals since those targets usually display a low water solubility and a need for functionalization strategies in organic solvents.

4. Conclusions

In summary, we developed a *de novo* synthesis strategy for an SMX derivative (SMXder) with a newly introduced thiol moiety connected to the isoxazole ring *via* a linker. We used SMXder together with a 1,11-bis(maleimido)-3,6,9-trioxaundecane linker for site-directed coupling onto PEG hydrogel microparticles bearing thiol moieties. We demonstrated the successful coupling and the undiminished structural integrity of the hydrogel microparticles by quantitative fluorescence analysis of labelled SMXder, differential FT-IR spectroscopy, bright field microscopy and RICM. Although we did not determine the absolute number of available SMXder molecules on the hydrogel microparticle surface, we could demonstrate a saturation of homogeneously distributed SMXder. This work represents a groundwork to develop a biosensor detection technique for sulfonamide antibiotics based on the recently published soft colloidal probe (SCP) principle. Since the introduction of sulfonamide antibiotics in the environment and their resulting accumulation pose a major threat to natural ecosystems and human health, there is an urgent need to monitor their environmental distribution.[8,19,24,25,44–46] Besides their very specific biosensing applications, functional microparticles can also be used in a different context such as pull-down assays or in screenings for unknown binding partners. With our work we showed that through modification of the target molecule and *de novo* synthesis and by choosing specific linkers, functional microparticles can be generated, showing options for a broad spectrum of different molecules.

Author contributions

Veronika Riedl: conceptualization, investigation, formal analysis, writing – original draft, and editing. Matthias Portius: conceptualization, investigation, formal analysis, writing – original draft, and editing. Lara Heiser: investigation and formal analysis. Philipp Riedl: investigation, formal analysis, and writing – editing. Torsten Jakob: investigation, formal analysis, and writing – editing. Rosa Gehring: investigation and formal analysis. Thorsten Berg: conceptualization and writing – editing. Tilo Pompe: conceptualization, writing – original draft, and editing.

Conflicts of interest

There are no conflicts to declare.

Acknowledgements

T. P. acknowledges the support from BMWK and SAB within the STARK program (project no. 46SKD023X). The access to the BioImaging Core Facility (Faculty of Life Sciences, Leipzig University) supported by a grant from DFG (INST 268/394-1 FUGG) to T. P. is gratefully acknowledged.

Notes and references

1 P. Huovinen, L. Sundström, G. Swedberg and O. Sköld, *Antimicrob. Agents Chemother.*, 1995, **39**, 279–289.
2 W. Baran, E. Adamek, J. Ziemiańska and A. Sobczak, *J. Hazard. Mater.*, 2011, **196**, 1–15.
3 P. A. Masters, T. A. O'Bryan, J. Zurlo, D. Q. Miller and N. Joshi, *Arch. Intern. Med.*, 2003, **163**, 402.
4 D. Fernández-Villa, M. R. Aguilar and L. Rojo, *Int. J. Mol. Sci.*, 2019, **20**, 4996.
5 R. Gothwal and T. Shashidhar, *Clean: Soil, Air, Water*, 2015, **43**, 479–489.
6 K. Hruska and M. Franek, *Vet. Med.*, 2012, **57**, 1–35.
7 L. Kergoat, P. Besse-Hoggan, M. Leremboure, J. Beguet, M. Devers, F. Martin-Laurent, M. Masson, S. Morin, A. Roinat, S. Pesce and C. Bonnineau, *Front. Microbiol.*, 2021, **12**, 643719.
8 J. Zhou, X. Yun, J. Wang, Q. Li and Y. Wang, *Toxicol. Rep.*, 2022, **9**, 534–540.
9 World Health Organization, **https://www.who.int/news-room/fact-sheets/detail/antibiotic-resistance**, (accessed April 2023).
10 L. G. Cortes, D. Marinov, I. Sanseverino, A. N. Cuenca, M. Niegowska, E. P. Rodriguez and T. Lettieri, *JRC Technical Report: Selection of substances for the 3rd Watch List under WFD*, 2020.
11 V. Goulas, T. Anisimova Andreou, C. Angastinioti Moditi and O. Tzamaloukas, *J. Anim. Feed Sci.*, 2014, **23**, 185–189.
12 M. Seifrtová, L. Nováková, C. Lino, A. Pena and P. Solich, *Anal. Chim. Acta*, 2009, **649**, 158–179.
13 W. M. M. Mahmoud, N. D. H. Khaleel, G. M. Hadad, R. A. Abdel-Salam, A. Haiß and K. Kümmerer, *Clean: Soil, Air, Water*, 2013, **41**, 907–916.
14 X. Liang, C. Li, J. Zhu, X. Song, W. Yu, J. Zhang, S. Zhang, J. Shen and Z. Wang, *Anal. Chim. Acta*, 2019, **1050**, 139–145.
15 P. S. Peixoto, P. H. Carvalho, A. Machado, L. Barreiros, A. A. Bordalo, H. P. Oliveira and M. A. Segundo, *Chemosensors*, 2022, **10**, 25.
16 L. del Torno-de Román, M. Asunción Alonso-Lomillo, O. Domínguez-Renedo and M. Julia Arcos-Martínez, *Sens. Actuators, B*, 2016, **227**, 48–53.
17 A. Ait Lahcen and A. Amine, *Anal. Lett.*, 2018, **51**, 424–441.
18 T. Jamshaid, E. T. Tenório-Neto, A. Baraket, N. Lebaz, A. Elaissari, A. Sanchís, J.-P. Salvador, M.-P. Marco, J. Bausells, A. Errachid and N. Zine, *Biosensors*, 2020, **10**, 43.
19 D. Pussak, M. Behra, S. Schmidt and L. Hartmann, *Soft Matter*, 2012, **8**, 1664–1672.

20 D. Pussak, D. Ponader, S. Mosca, S. V. Ruiz, L. Hartmann and S. Schmidt, *Angew. Chem., Int. Ed.*, 2013, **52**, 6084–6087.
21 A. K. Strzelczyk, H. Wang, A. Lindhorst, J. Waschke, T. Pompe, C. Kropf, B. Luneau and S. Schmidt, *Gels*, 2017, **3**, 31.
22 S. Martin, H. Wang, L. Hartmann, T. Pompe and S. Schmidt, *Phys. Chem. Chem. Phys.*, 2015, **17**, 3014–3018.
23 K. L. Johnson, K. Kendall and A. D. Roberts, *Proc. R. Soc. A*, 1971, **324**, 301–313.
24 D. Rettke, F. Seufert, J. Döring, K. Ostermann, D. Wilms, S. Schmidt and T. Pompe, *Biosens. Bioelectron.*, 2021, **192**, 113506.
25 D. Rettke, J. Döring, S. Martin, T. Venus, I. Estrela-Lopis, S. Schmidt, K. Ostermann and T. Pompe, *Biosens. Bioelectron.*, 2020, **165**, 112262.
26 G. Prasannamedha and P. S. Kumar, *J. Cleaner Prod.*, 2020, **250**, 119553.
27 E. E. Connor, *Primary Care Update OB/GYNS*, 1998, **5**, 32–35.
28 A. Ovung and J. Bhattacharyya, *Biophys. Rev.*, 2021, **13**, 259–272.
29 S. Mondal, *Synth. Commun.*, 2021, **51**, 1023–1044.
30 S. Fuse, T. Morita and H. Nakamura, *Synthesis*, 2017, 2351–2360.
31 A. R. Sekirnik née Measures, D. S. Hewings, N. H. Theodoulou, L. Jursins, K. R. Lewendon, L. E. Jennings, T. P. C. Rooney, T. D. Heightman and S. J. Conway, *Angew. Chem., Int. Ed.*, 2016, **55**, 8353–8357.
32 K. K. Pasunooti, B. Banerjee, T. Yap, Y. Jiang and C.-F. Liu, *Org. Lett.*, 2015, **17**, 6094–6097.
33 D. Rettke, C. Danneberg, T. A. Neuendorf, S. Kühn, J. Friedrichs, N. Hauck, C. Werner, J. Thiele and T. Pompe, *J. Mater. Chem. B*, 2022, **10**, 1663–1674.
34 C. T. Rueden, J. Schindelin, M. C. Hiner, B. E. DeZonia, A. E. Walter, E. T. Arena and K. W. Eliceiri, *BMC Bioinf.*, 2017, **18**, 529.
35 J. Schindelin, I. Arganda-Carreras, E. Frise, V. Kaynig, M. Longair, T. Pietzsch, S. Preibisch, C. Rueden, S. Saalfeld, B. Schmid, J.-Y. Tinevez, D. J. White, V. Hartenstein, K. Eliceiri, P. Tomancak and A. Cardona, *Nat. Methods*, 2012, **9**, 676–682.
36 M. Linkert, C. T. Rueden, C. Allan, J.-M. Burel, W. Moore, A. Patterson, B. Loranger, J. Moore, C. Neves, D. MacDonald, A. Tarkowska, C. Sticco, E. Hill, M. Rossner, K. W. Eliceiri and J. R. Swedlow, *J. Cell Biol.*, 2010, **189**, 777–782.
37 M.-M. Zhan, Y. Yang, J. Luo, X.-X. Zhang, X. Xiao, S. Li, K. Cheng, Z. Xie, Z. Tu and C. Liao, *Eur. J. Med. Chem.*, 2018, **143**, 724–731.
38 S. Sowmiah, J. M. S. S. Esperança, L. P. N. Rebelo and C. A. M. Afonso, *Org. Chem. Front.*, 2018, **5**, 453–493.
39 X. Deng and N. S. Mani, *Green Chem.*, 2006, **8**, 835.
40 D. Rettke, J. Döring, S. Martin, T. Venus, I. Estrela-Lopis, S. Schmidt, K. Ostermann and T. Pompe, *Biosens. Bioelectron.*, 2020, **165**, 112262.
41 D. Hernández, L. Lazo, L. Valdés, L. C. de Ménorval, Z. Rozynek and A. Rivera, *Appl. Clay Sci.*, 2018, **161**, 395–403.
42 K. J. Hartauer and J. K. Guillory, *Pharm. Res.*, 1989, **6**, 608–611.
43 S. Schmidt, H. Wang, D. Pussak, S. Mosca and L. Hartmann, *Beilstein J. Org. Chem.*, 2015, **11**, 720–729.
44 S. Martin, H. Wang, L. Hartmann, T. Pompe and S. Schmidt, *Phys. Chem. Chem. Phys.*, 2015, **17**, 3014–3018.
45 D. Pussak, D. Ponader, S. Mosca, T. Pompe, L. Hartmann and S. Schmidt, *Langmuir*, 2014, **30**, 6142–6150.
46 D. G. J. Larsson and C.-F. Flach, *Nat. Rev. Microbiol.*, 2022, **20**, 257–269.

